Accurate linearization of non-gray radiation heat transfer

The internal fractional function revisited

John H. Lienhard V

Rohsenow Kendall Heat Transfer Lab
Massachusetts Institute of Technology
Cambridge MA 02139-4307 USA

PRTEC 2019, Maui, 15 December 2019

Net radiation exchange

Small object (1) in large isothermal surrounds (2)

The net radiation leaving this surface is

$$q_{\text{net}} = \sigma\varepsilon(T_1)T_1^4 - \sigma\alpha(T_1, T_2)T_2^4 \tag{1}$$

Total hemispherical emissivity and absorptivity

$$\varepsilon(T_1) = \frac{1}{\sigma T_1^4}\int_0^\infty \alpha(\lambda, T_1)e_{\lambda,b}(T_1)\,d\lambda$$

$$\alpha(T_1, T_2) = \frac{1}{\sigma T_2^4}\int_0^\infty \alpha(\lambda, T_1)e_{\lambda,b}(T_2)\,d\lambda$$

Net radiation exchange

Small object (1) in large isothermal surrounds (2)

The net radiation leaving this surface is

$$q_{\text{net}} = \sigma\varepsilon(T_1)T_1^4 - \sigma\alpha(T_1, T_2)T_2^4 \tag{1}$$

Total hemispherical emissivity and absorptivity

$$\varepsilon(T_1) = \frac{1}{\sigma T_1^4}\int_0^\infty \alpha(\lambda, T_1)e_{\lambda,b}(T_1)\,d\lambda$$

$$\alpha(T_1, T_2) = \frac{1}{\sigma T_2^4}\int_0^\infty \alpha(\lambda, T_1)e_{\lambda,b}(T_2)\,d\lambda$$

If $T_2 \to T_1$ then $\alpha(T_1, T_2) \to \varepsilon(T_1)$, but ...

Non-gray error

Linearization about T_1 for small temperature differences

The slope as $T_2 \to T_1$ is different when $d\alpha/dT_2 \neq 0$.

$$\alpha(T_1, T_2)\, T_2^4 \approx \alpha(T_1, T_1)\, T_1^4 + \frac{d}{dT_2}\Big(\alpha(T_1, T_2)\, T_2^4\Big)\Big|_{T_1} (T_2 - T_1)$$

$$= \varepsilon(T_1)\, T_1^4 + 4T_1^3 \left[\varepsilon(T_1) + \frac{T_1}{4} \frac{d\alpha}{dT_2}\Big|_{T_1}\right](T_2 - T_1)$$

Non-gray error

Linearization about T_1 for small temperature differences

The slope as $T_2 \to T_1$ is different when $d\alpha/dT_2 \neq 0$.

$$\begin{aligned}\alpha(T_1,T_2)\,T_2^4 &\approx \alpha(T_1,T_1)\,T_1^4 + \frac{d}{dT_2}\Big(\alpha(T_1,T_2)\,T_2^4\Big)\Big|_{T_1}(T_2-T_1)\\ &= \varepsilon(T_1)\,T_1^4 + 4T_1^3\left[\varepsilon(T_1) + \frac{T_1}{4}\,\frac{d\alpha}{dT_2}\Big|_{T_1}\right](T_2-T_1)\end{aligned}$$

Thus,

$$q_{\text{net}} \approx 4\sigma T_1^3\left[\varepsilon(T_1) + \frac{T_1}{4}\,\frac{d\alpha}{dT_2}\Big|_{T_1}\right](T_1-T_2) \tag{2}$$

Non-gray error

Linearization about T_1 for small temperature differences

The slope as $T_2 \to T_1$ is different when $d\alpha/dT_2 \neq 0$.

$$\begin{aligned}\alpha(T_1, T_2)\, T_2^4 &\approx \alpha(T_1, T_1)\, T_1^4 + \frac{d}{dT_2}\Big(\alpha(T_1, T_2)\, T_2^4\Big)\Big|_{T_1} (T_2 - T_1) \\ &= \varepsilon(T_1)\, T_1^4 + 4T_1^3 \left[\varepsilon(T_1) + \frac{T_1}{4} \frac{d\alpha}{dT_2}\Big|_{T_1} \right] (T_2 - T_1)\end{aligned}$$

Thus,

$$q_{\text{net}} \approx 4\sigma T_1^3 \left[\varepsilon(T_1) + \frac{T_1}{4} \frac{d\alpha}{dT_2}\Big|_{T_1} \right] (T_1 - T_2) \tag{2}$$

For a gray (or black) surface, $d\alpha/dT_2 = 0$, so: $q_{\text{net}} \approx 4\sigma \varepsilon(T_1)\, T_1^3 \Delta T$.

Background

External and internal emissivities

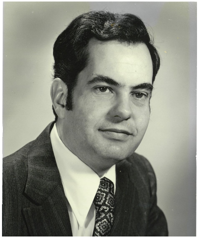

DK Edwards (1932–2009)

UCLA 1959-1981, UCI 1981-1991
ASME Heat Transfer Memorial Award (1973)

In his work on radiative property measurements, he studied the failure of gray-body approximations at even small ΔT

- Edwards suggested the *internal radiation fractional function* for linearizing net heat flux between surfaces at small ΔT. Appears in several textbooks by Edwards and his coworkers.
- Internal to a spacecraft: small ΔT
- External to a spacecraft: large ΔT

Internal Fractional Function

Linearization about T_1 for small temperature differences

Edwards defined the *internal* total hemispherical emissivity as

$$\varepsilon^i(T_1) \equiv \lim_{T_2 \to T_1} \frac{\varepsilon(T_1)\sigma T_1^4 - \alpha(T_1, T_2)\sigma T_2^4}{\sigma T_1^4 - \sigma T_2^4} = \lim_{T_2 \to T_1} \frac{\displaystyle\int_0^\infty \alpha(\lambda, T_1)\frac{\partial}{\partial T_2} e_{\lambda,b}(T_2)\, d\lambda}{4\sigma T_2^3} \qquad (3)$$

Internal Fractional Function

Linearization about T_1 for small temperature differences

Edwards defined the *internal* total hemispherical emissivity as

$$\varepsilon^i(T_1) \equiv \lim_{T_2 \to T_1} \frac{\varepsilon(T_1)\sigma T_1^4 - \alpha(T_1, T_2)\sigma T_2^4}{\sigma T_1^4 - \sigma T_2^4} = \lim_{T_2 \to T_1} \frac{\displaystyle\int_0^\infty \alpha(\lambda, T_1) \frac{\partial}{\partial T_2} e_{\lambda,b}(T_2)\, d\lambda}{4\sigma T_2^3} \tag{3}$$

Thus, when T_2 is not too much different from T_1

$$q_{\text{net}} \approx \varepsilon^i(T_1)\, 4\sigma T_1^3 (T_1 - T_2) \tag{4}$$

Internal Fractional Function

Linearization about T_1 for small temperature differences

Edwards defined the *internal* total hemispherical emissivity as

$$\varepsilon^i(T_1) \equiv \lim_{T_2 \to T_1} \frac{\varepsilon(T_1)\sigma T_1^4 - \alpha(T_1, T_2)\sigma T_2^4}{\sigma T_1^4 - \sigma T_2^4} = \lim_{T_2 \to T_1} \frac{\displaystyle\int_0^\infty \alpha(\lambda, T_1) \frac{\partial}{\partial T_2} e_{\lambda,b}(T_2)\, d\lambda}{4\sigma T_2^3} \tag{3}$$

Thus, when T_2 is not too much different from T_1

$$q_{\text{net}} \approx \varepsilon^i(T_1)\, 4\sigma T_1^3 (T_1 - T_2) \tag{4}$$

with

$$\varepsilon^i(T) = \frac{1}{4\sigma T^3} \int_0^\infty \alpha(\lambda, T) \frac{\partial e_{\lambda,b}}{\partial T}\, d\lambda = \int_0^1 \alpha(\lambda, T)\, d f_i(\lambda T) \tag{5}$$

where the **internal fractional function** is

$$f_i(\lambda T) \equiv \frac{1}{4\sigma T^3} \int_0^\lambda \frac{\partial e_{\lambda,b}}{\partial T}\, d\lambda \tag{6}$$

External Fractional Function

What we usually called the radiation fractional function

The fraction of blackbody radiation between wavelengths of 0 and λ is

$$\begin{aligned} f(\lambda T) &= \frac{1}{\sigma T^4} \int_0^\lambda e_{\lambda,b} \, d\lambda \\ &= 1 - \frac{90}{\pi^4} \zeta(c_2/\lambda T, 4) \end{aligned} \tag{7}$$

where $\zeta(X, s)$ is the incomplete zeta function. (Details in paper.)

External Fractional Function

What we usually called the radiation fractional function

The fraction of blackbody radiation between wavelengths of 0 and λ is

$$\begin{aligned} f(\lambda T) &= \frac{1}{\sigma T^4} \int_0^{\lambda} e_{\lambda,b}\, d\lambda \\ &= 1 - \frac{90}{\pi^4}\, \zeta(c_2/\lambda T, 4) \end{aligned} \tag{7}$$

where $\zeta(X, s)$ is the incomplete zeta function. (Details in paper.)

The *external* total hemispherical emissivity is

$$\varepsilon(T) = \int_0^1 \alpha(\lambda, T)\, df(\lambda T)$$

External Fractional Function

What we usually called the radiation fractional function

The fraction of blackbody radiation between wavelengths of 0 and λ is

$$f(\lambda T) = \frac{1}{\sigma T^4} \int_0^\lambda e_{\lambda,b}\, d\lambda$$
$$= 1 - \frac{90}{\pi^4}\, \zeta(c_2/\lambda T, 4) \qquad (7)$$

where $\zeta(X, s)$ is the incomplete zeta function. (Details in paper.)

The *external* total hemispherical emissivity is

$$\varepsilon(T) = \int_0^1 \alpha(\lambda, T)\, d f(\lambda T)$$

From these relationships, one can show that

$$f_i(\lambda T) - f(\lambda T) = F(X) = \frac{15}{4\pi^4} \frac{X^4}{e^X - 1} \qquad (8)$$

where $X \equiv c_2/\lambda T$.

$f_i(\lambda T) - f(\lambda T) = F(X)$

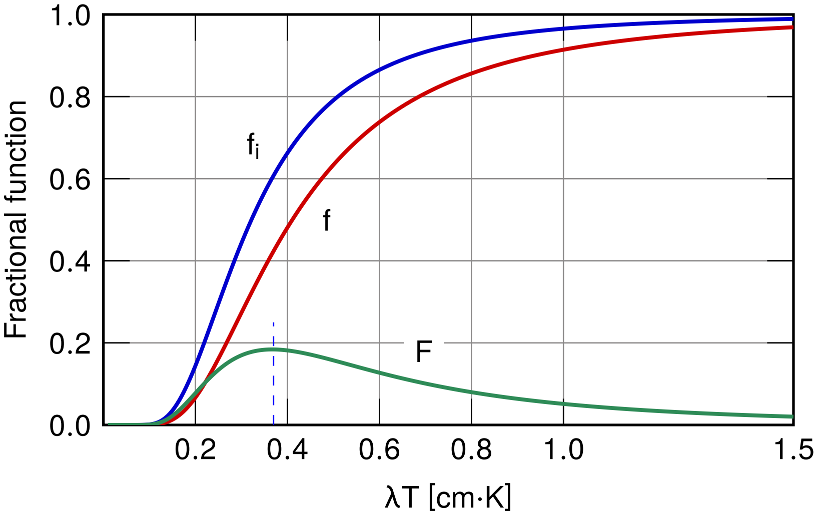

$f_i(\lambda T) - f(\lambda T) = F(X)$ $X = c_2/\lambda T$

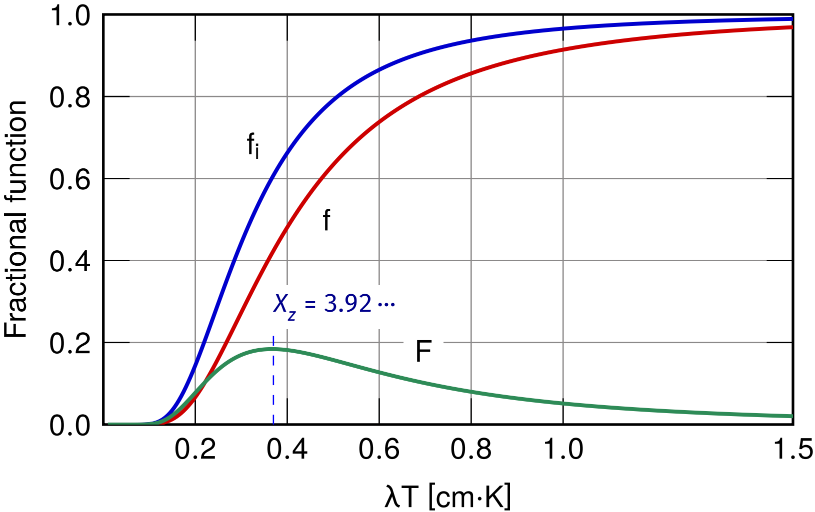

Difference between external and internal emissivities

$$\varepsilon - \varepsilon^i = \int_0^1 \alpha(\lambda, T)\, df(\lambda T) - \int_0^1 \alpha(\lambda, T)\, df_i(\lambda T) = \int_0^\infty \alpha(\lambda, T) \frac{dF}{dX}\, dX$$

Difference between external and internal emissivities

$$
\begin{aligned}
\varepsilon - \varepsilon^{i} &= \int_0^1 \alpha(\lambda, T)\, df(\lambda T) - \int_0^1 \alpha(\lambda, T)\, df_i(\lambda T) = \int_0^\infty \alpha(\lambda, T) \frac{dF}{dX}\, dX \\
&= \int_0^{X_z} \alpha(\lambda, T) \frac{dF}{dX}\, dX + \int_{X_z}^\infty \alpha(\lambda, T) \frac{dF}{dX}\, dX
\end{aligned}
$$

where $dF/dX = 0$ at $X_z = 3.92069$.

Difference between external and internal emissivities

$$\varepsilon - \varepsilon^i = \int_0^1 \alpha(\lambda,T)\,df(\lambda T) - \int_0^1 \alpha(\lambda,T)\,df_i(\lambda T) = \int_0^\infty \alpha(\lambda,T)\frac{dF}{dX}\,dX$$

$$= \int_0^{X_z} \alpha(\lambda,T)\frac{dF}{dX}\,dX + \int_{X_z}^\infty \alpha(\lambda,T)\frac{dF}{dX}\,dX$$

where $dF/dX = 0$ at $X_z = 3.92069$. Because $dF/dX > 0$ for $X < X_z$ and < 0 for $X > X_z$:

$$\varepsilon - \varepsilon^i \leqslant \int_0^{X_z} \frac{dF}{dX}\,dX = F(X_z) \quad \text{if } \varepsilon - \varepsilon^i > 0, \text{ and}$$

$$\varepsilon^i - \varepsilon \leqslant \int_\infty^{X_z} \frac{dF}{dX}\,dX = F(X_z) \quad \text{if } \varepsilon^i - \varepsilon > 0$$

Difference between external and internal emissivities

$$\varepsilon - \varepsilon^i = \int_0^1 \alpha(\lambda, T)\, df(\lambda T) - \int_0^1 \alpha(\lambda, T)\, df_i(\lambda T) = \int_0^\infty \alpha(\lambda, T) \frac{dF}{dX}\, dX$$
$$= \int_0^{X_z} \alpha(\lambda, T) \frac{dF}{dX}\, dX + \int_{X_z}^\infty \alpha(\lambda, T) \frac{dF}{dX}\, dX$$

where $dF/dX = 0$ at $X_z = 3.92069$. Because $dF/dX > 0$ for $X < X_z$ and < 0 for $X > X_z$:

$$\varepsilon - \varepsilon^i \leqslant \int_0^{X_z} \frac{dF}{dX}\, dX = F(X_z) \quad \text{if } \varepsilon - \varepsilon^i > 0\text{, and}$$
$$\varepsilon^i - \varepsilon \leqslant \int_\infty^{X_z} \frac{dF}{dX}\, dX = F(X_z) \quad \text{if } \varepsilon^i - \varepsilon > 0$$

Evaluating

$$\boxed{\left|\varepsilon - \varepsilon^i\right| \leqslant 0.18400} \tag{9}$$

Model surfaces: Switch between $\alpha(\lambda) = 0$ and $\alpha(\lambda) = 1$ at $X_z = c_2/\lambda_z T = 3.92069$

Emissivities evaluated numerically

Case 1: 300 K surface, black for $\lambda_z \leqslant 12.23$ μm, but reflective on other wavelengths.

$$\varepsilon = 0.4177, \quad \varepsilon^i = 0.6017, \quad \text{and} \quad \varepsilon^i - \varepsilon = 0.1840 \tag{10}$$

Case 2: 300 K surface, black for 12.23 μm $\leqslant \lambda_z$, but reflective on other wavelengths:

$$\varepsilon = 0.5823, \quad \varepsilon^i = 0.3983, \quad \text{and} \quad \varepsilon - \varepsilon^i = 0.1840 \tag{11}$$

In both cases $\alpha(T_1, T_2)$ is a strong function of T_2.

Linearization of q_{net} about T_1 is less accurate than for T_m

Consider q_{net} for a black surface: T_1, eqn. (32); T_m, eqn. (33). $T_m = (T_1 + T_2)/2$

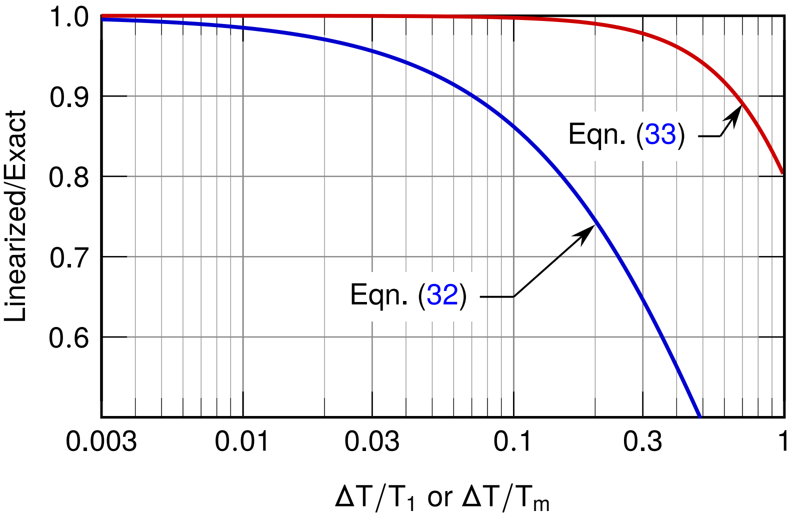

Linearization with internal emissivity

Linearize about $T_m = (T_1 + T_2)/2$

Linearization accuracy is also greater for a non-gray surface when using T_m, *but must include temperature dependence of* $\alpha(T_1, T_2)$.

- Linearization about T_1 is just Edward's definition: $q_{\text{net}} \approx \varepsilon^i(T_1)\, 4\sigma T_1^3 \Delta T$
  It is a first-order, single-step, Euler approximation.

Linearization with internal emissivity

Linearize about $T_m = (T_1 + T_2)/2$

Linearization accuracy is also greater for a non-gray surface when using T_m, *but must include temperature dependence of* $\alpha(T_1, T_2)$.

- Linearization about T_1 is just Edward's definition: $q_{\text{net}} \approx \varepsilon^i(T_1)\, 4\sigma T_1^3 \Delta T$
  It is a first-order, single-step, Euler approximation.
- Linearization about T_m is a second-order, single-step Runge-Kutta approximation. Calculation gives (details in paper)

$$\boxed{q_{\text{net}} \approx 4\varepsilon^i(T_m)\cdot\sigma T_m^3 \Delta T} \tag{12}$$

to an accuracy of $\mathbf{O}\left(\mathbf{\Delta T^3}\right)$.

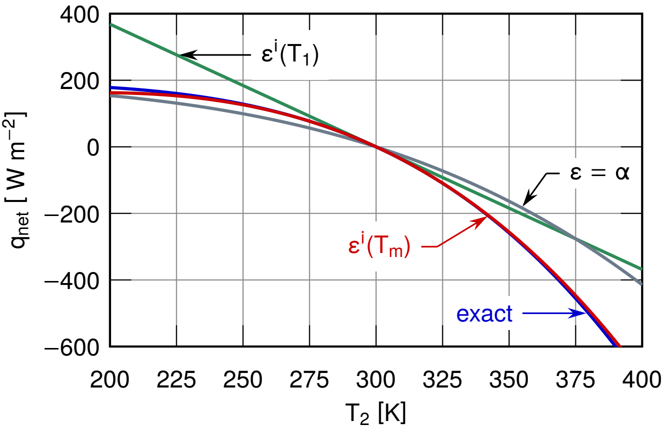

FIGURE 4. COMPARISON OF MODELS FOR q_{net} (300 K SURFACE, BLACK BELOW 12.23 µm)

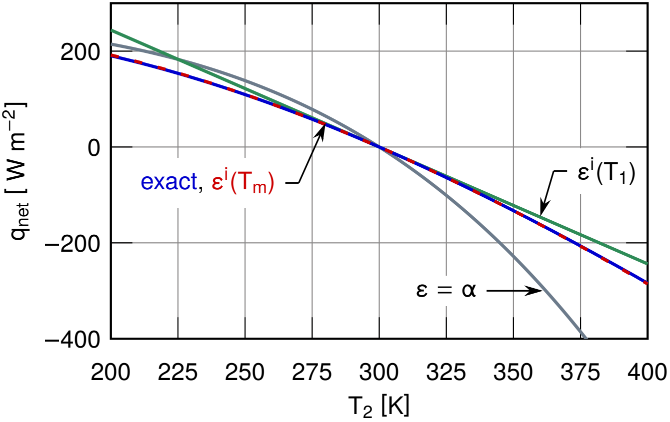

FIGURE 5. COMPARISON OF MODELS FOR q_{net} (300 K SURFACE, BLACK ABOVE 12.23 μm)

Polycrystalline alumina, normal emissivity

99.5% Al_2O_3, 6 mm thick, 1 μm roughness, T_1 = 823 K (Teodorescu and Jones, 2008)

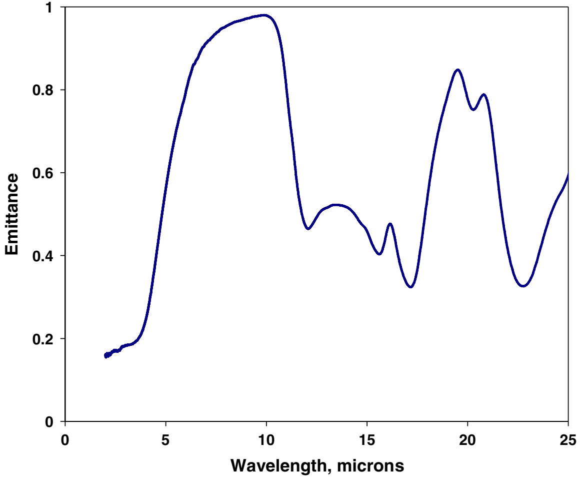

Polycrystalline alumina, normal emissivity

99.5% Al_2O_3, 6 mm thick, 1 μm roughness, T_1 = 823 K (Teodorescu and Jones, 2008)

Total, normal

$\varepsilon_n = 0.506$

$\varepsilon_n^i = 0.404$

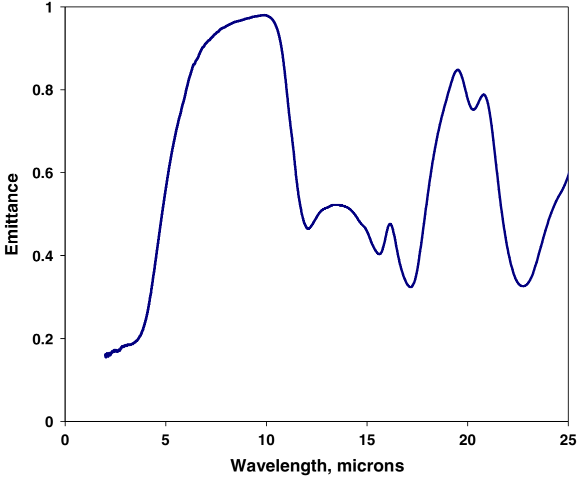

Polycrystalline alumina at T_1 = 823 K

$\varepsilon^i(T_m)$ provides much wider accuracy than $\varepsilon^i(T_1)$

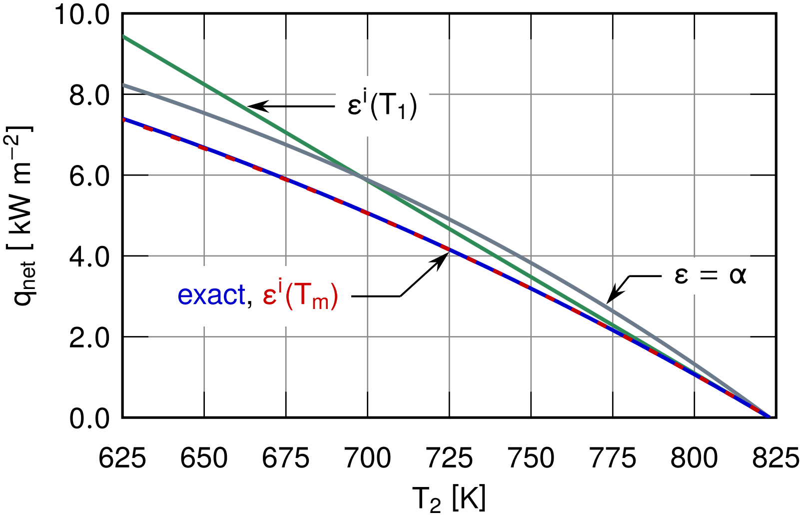

Platinum, T_1 = 373 K

Drude/Hagen-Rubens model for spectral hemispherical emissivity (Baehr & Stephan, 1998)

$$\varepsilon(\lambda, T) = 48.70\sqrt{\frac{r_e}{\lambda}}\left\{1 + \left[31.62 + 6.849\ln\left(\frac{r_e}{\lambda}\right)\right]\sqrt{\frac{r_e}{\lambda}} - 166.78\,\frac{r_e}{\lambda} + \cdots\right\}$$

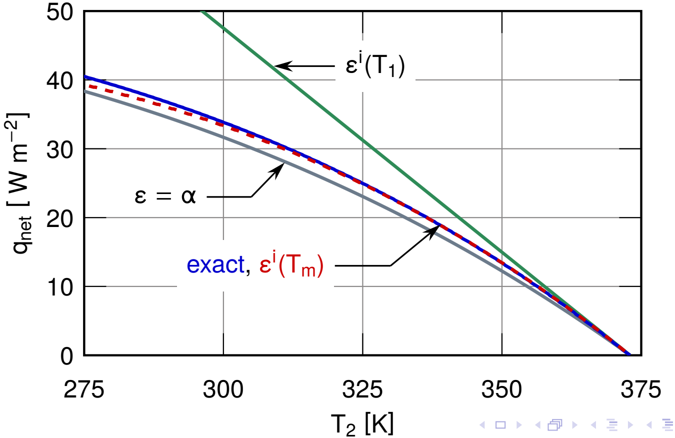

Model of spectrally selective surface

Similar to data for soft-anodized aluminum in Edwards' *Radiation Heat Transfer Notes*

$$\alpha(\lambda) = \begin{cases} \alpha_{\text{sw}} & \text{for } \lambda \leqslant \lambda_c \\ \alpha_{\text{lw}} & \text{for } \lambda > \lambda_c \end{cases}$$

Model of spectrally selective surface

Similar to data for soft-anodized aluminum in Edwards' *Radiation Heat Transfer Notes*

$$\alpha(\lambda) = \begin{cases} \alpha_{\text{sw}} & \text{for } \lambda \leqslant \lambda_c \\ \alpha_{\text{lw}} & \text{for } \lambda > \lambda_c \end{cases}$$

Can write

$$\varepsilon(T_1) = \alpha_{\text{sw}} f(\lambda_c T_1) + \alpha_{\text{lw}} \left[1 - f(\lambda_c T_1)\right] = \alpha_{\text{sw}} + \frac{90}{\pi^4} \Delta\alpha\, \zeta(X_{c,1}, 4)$$

where $X_{c,1} = c_2/\lambda_c T_1$ and $\Delta\alpha = \alpha_{\text{lw}} - \alpha_{\text{sw}}$.

Model of spectrally selective surface

Similar to data for soft-anodized aluminum in Edwards' *Radiation Heat Transfer Notes*

$$\alpha(\lambda) = \begin{cases} \alpha_{\mathrm{sw}} & \text{for } \lambda \leqslant \lambda_c \\ \alpha_{\mathrm{lw}} & \text{for } \lambda > \lambda_c \end{cases}$$

Can write

$$\varepsilon(T_1) = \alpha_{\mathrm{sw}} f(\lambda_c T_1) + \alpha_{\mathrm{lw}} \left[1 - f(\lambda_c T_1)\right] = \alpha_{\mathrm{sw}} + \frac{90}{\pi^4} \Delta\alpha\, \zeta(X_{c,1}, 4)$$

where $X_{c,1} = c_2/\lambda_c T_1$ and $\Delta\alpha = \alpha_{\mathrm{lw}} - \alpha_{\mathrm{sw}}$. Further,

$$\varepsilon^i(T_m) = \alpha_{\mathrm{sw}} + \Delta\alpha \left[\frac{90}{\pi^4} \zeta(X_{c,m}, 4) - F(X_{c,m}) \right]$$

where $X_{c,m} = c_2/\lambda_c T_m$.

Model of spectrally selective surface

Similar to data for soft-anodized aluminum in Edwards' *Radiation Heat Transfer Notes*

$$\alpha(\lambda) = \begin{cases} \alpha_{\text{sw}} & \text{for } \lambda \leqslant \lambda_c \\ \alpha_{\text{lw}} & \text{for } \lambda > \lambda_c \end{cases}$$

Can write

$$\varepsilon(T_1) = \alpha_{\text{sw}} f(\lambda_c T_1) + \alpha_{\text{lw}} \left[1 - f(\lambda_c T_1)\right] = \alpha_{\text{sw}} + \frac{90}{\pi^4} \Delta\alpha\, \zeta(X_{c,1}, 4)$$

where $X_{c,1} = c_2/\lambda_c T_1$ and $\Delta\alpha = \alpha_{\text{lw}} - \alpha_{\text{sw}}$. Further,

$$\varepsilon^i(T_m) = \alpha_{\text{sw}} + \Delta\alpha \left[\frac{90}{\pi^4} \zeta(X_{c,m}, 4) - F(X_{c,m}) \right]$$

where $X_{c,m} = c_2/\lambda_c T_m$. Finally,

$$\alpha(T_1, T_2) = \alpha_{\text{sw}} + \frac{90}{\pi^4} \Delta\alpha\, \zeta(X_{c,2}, 4)$$

with $X_{c,2} = c_2/\lambda_c T_2$. Impact of selectivity greatest when X_c and X_z are close.

Soft anodized aluminum at T_1 = 360 K with T_2 = 290 K

Selective solar reflector: $\alpha_{sw} = 0.1$, $\alpha_{lw} = 0.85$, and $\lambda_c = 7$ µm. Heat flux in W/m^2.

$\varepsilon(T_1)$	$\varepsilon^i(T_1)$	$\varepsilon^i(T_m)$	$\alpha(T_1, T_2)$
0.7258	0.6237	0.6807	0.7964
q_{gray}	$q_{\text{int},\,T_1}$	$q_{\text{int},\,T_m}$	q_{exact}
400.2	462.1	371.0	371.8

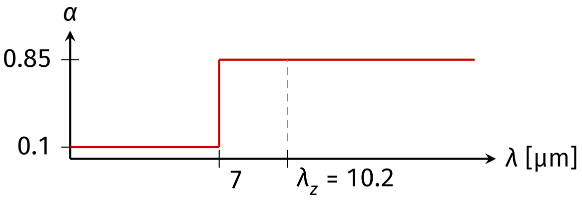

Radiation thermal resistance

$\varepsilon^i(T_m)$ should be used for this linearization

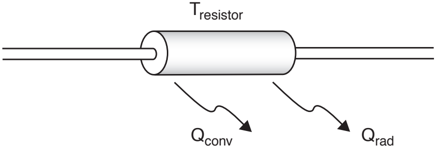

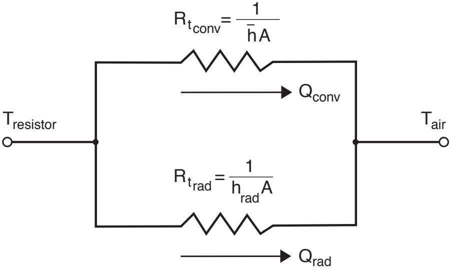

$$
\begin{aligned}
R_{t_{\text{rad}}} &= \frac{1}{h_{\text{rad}}A} \\
&= \frac{1}{4\varepsilon\sigma T_m^3 A} \\
&= \frac{1}{4\,\varepsilon^i(T_m)\,\sigma T_m^3 A}
\end{aligned}
$$

Summary

$\varepsilon^i(T_m)$ is useful for radiation thermal resistance

Edwards and others have suggested $\varepsilon^i(T_1)$ for non-gray exchange in enclosures with modest ΔT, to provide a correct linearization of q_{net}.

Summary

$\varepsilon^i(T_m)$ is useful for radiation thermal resistance

Edwards and others have suggested $\varepsilon^i(T_1)$ for non-gray exchange in enclosures with modest ΔT, to provide a correct linearization of q_{net}.

1. Theory and examples for several non-gray materials show that the gray-body approximation gives the wrong slope for heat flux as $T_2 \to T_1$.

Summary

$\varepsilon^i(T_m)$ is useful for radiation thermal resistance

Edwards and others have suggested $\varepsilon^i(T_1)$ for non-gray exchange in enclosures with modest ΔT, to provide a correct linearization of q_{net}.

1. Theory and examples for several non-gray materials show that the gray-body approximation gives the wrong slope for heat flux as $T_2 \to T_1$.
2. $\left|\varepsilon(T_1) - \varepsilon^i(T_1)\right| \leqslant 0.18400$

Summary

$\varepsilon^i(T_m)$ is useful for radiation thermal resistance

Edwards and others have suggested $\varepsilon^i(T_1)$ for non-gray exchange in enclosures with modest ΔT, to provide a correct linearization of q_{net}.

1. Theory and examples for several non-gray materials show that the gray-body approximation gives the wrong slope for heat flux as $T_2 \to T_1$.
2. $\left|\varepsilon(T_1) - \varepsilon^i(T_1)\right| \leqslant 0.18400$
3. ε^i should be evaluated at the mean temperature, T_m, not T_1 as has often been suggested. T_m gives a truncation error in q_{net} of $O(\Delta T^3)$.

Summary

$\varepsilon^i(T_m)$ is useful for radiation thermal resistance

Edwards and others have suggested $\varepsilon^i(T_1)$ for non-gray exchange in enclosures with modest ΔT, to provide a correct linearization of q_{net}.

1. Theory and examples for several non-gray materials show that the gray-body approximation gives the wrong slope for heat flux as $T_2 \to T_1$.
2. $\left|\varepsilon(T_1) - \varepsilon^i(T_1)\right| \leqslant 0.18400$
3. ε^i should be evaluated at the mean temperature, T_m, not T_1 as has often been suggested. T_m gives a truncation error in q_{net} of $O(\Delta T^3)$.
4. $\varepsilon^i(T_m)$ should be used for radiation thermal resistances of non-gray surfaces. Agreement excellent $T_2/T_1 = 1 \pm 30\%$ or more.

Summary

$\varepsilon^i(T_m)$ is useful for radiation thermal resistance

Edwards and others have suggested $\varepsilon^i(T_1)$ for non-gray exchange in enclosures with modest ΔT, to provide a correct linearization of q_{net}.

1. Theory and examples for several non-gray materials show that the gray-body approximation gives the wrong slope for heat flux as $T_2 \to T_1$.
2. $\left|\varepsilon(T_1) - \varepsilon^i(T_1)\right| \leqslant 0.18400$
3. ε^i should be evaluated at the mean temperature, T_m, not T_1 as has often been suggested. T_m gives a truncation error in q_{net} of $O(\Delta T^3)$.
4. $\varepsilon^i(T_m)$ should be used for radiation thermal resistances of non-gray surfaces. Agreement excellent $T_2/T_1 = 1 \pm 30\%$ or more.
5. Calculations involving both the internal and external fractional functions can be conveniently implemented using the incomplete zeta function.

Thank you!

To read more, see this paper:

J. H. Lienhard V, “Linearization of Non-gray Radiation Exchange: The Internal Fractional Function Reconsidered,” *J. Heat Transfer*, **141**(5):052701, May 2019.

OPEN ACCESS: https://doi.org/10.1115/1.4042158

Supplementary slides

Second-order, single-step, Runge-Kutta approximation

$$q_{\text{net}} = Y(T_2) = \sigma\varepsilon(T_1)T_1^4 - \sigma\alpha(T_1, T_2)T_2^4$$

Second-order, single-step, Runge-Kutta approximation

$$q_{\text{net}} = Y(T_2) = \sigma\varepsilon(T_1)T_1^4 - \sigma\alpha(T_1, T_2)T_2^4$$

A second-order Runge-Kutta method works from T_m with expansions toward both T_1 and T_2, subtracting the former from the latter:

$$Y(T_2) = Y(T_m) + Y'(T_m)\frac{\delta T}{2} + Y''(T_m)\frac{\delta T^2}{8} + O(\delta T^3)$$
$$Y(T_1) = Y(T_m) - Y'(T_m)\frac{\delta T}{2} + Y''(T_m)\frac{\delta T^2}{8} - O(\delta T^3)$$

Subtract

$$Y(T_2) = Y(T_1) + Y'(T_m) \cdot \delta T + O(\delta T^3)$$
$$Y(T_2) \approx Y'(T_m) \cdot \delta T$$

Second-order, single-step, Runge-Kutta approximation

$$q_{\text{net}} = Y(T_2) = \sigma\varepsilon(T_1)T_1^4 - \sigma\alpha(T_1, T_2)T_2^4$$

A second-order Runge-Kutta method works from T_m with expansions toward both T_1 and T_2, subtracting the former from the latter:

$$Y(T_2) = Y(T_m) + Y'(T_m)\frac{\delta T}{2} + Y''(T_m)\frac{\delta T^2}{8} + O(\delta T^3)$$
$$Y(T_1) = Y(T_m) - Y'(T_m)\frac{\delta T}{2} + Y''(T_m)\frac{\delta T^2}{8} - O(\delta T^3)$$

Subtract

$$Y(T_2) = Y(T_1) + Y'(T_m) \cdot \delta T + O(\delta T^3)$$
$$Y(T_2) \approx Y'(T_m) \cdot \delta T$$

$$Y'(T_m) = -\frac{d}{dT}\left(\sigma T^4 \alpha(T_1, T)\right)\Big|_{T_m} = \cdots = -4\sigma T_m^3 \cdot \varepsilon^i(T_m)$$

Incomplete zeta function and $f(\lambda T)$

$$f(\lambda T) = \frac{1}{\sigma T^4} \int_0^\lambda \frac{2\pi h c_o^2}{\lambda^5 \left[\exp(hc_o/k_B T\lambda) - 1\right]} \, d\lambda = \frac{1}{\sigma T^4} \frac{2\pi k_B^4 T^4}{h^3 c_o^2} \int_{c_2/\lambda T}^{\infty} \frac{t^3}{e^t - 1} \, dt$$

Incomplete zeta function and $f(\lambda T)$

$$f(\lambda T) = \frac{1}{\sigma T^4} \int_0^\lambda \frac{2\pi h c_o^2}{\lambda^5 \left[\exp(hc_o/k_B T\lambda) - 1\right]} \, d\lambda = \frac{1}{\sigma T^4} \frac{2\pi k_B^4 T^4}{h^3 c_o^2} \int_{c_2/\lambda T}^{\infty} \frac{t^3}{e^t - 1} \, dt$$

When $\lambda T \to \infty$, $f = 1$ and so

$$\sigma T^4 = \frac{2\pi k_B^4 T^4}{h^3 c_o^2} \underbrace{\int_0^\infty \frac{t^3}{e^t - 1} \, dt}_{\equiv \zeta(4)\Gamma(4)}$$

where $\Gamma(4) = 3!$ and $\zeta(4)$ is the Riemann zeta function (Euler: $\zeta(4) = \pi^4/90$).

Incomplete zeta function and $f(\lambda T)$

$$f(\lambda T) = \frac{1}{\sigma T^4} \int_0^{\lambda} \frac{2\pi h c_o^2}{\lambda^5 \left[\exp(hc_o/k_B T\lambda) - 1\right]} \, d\lambda = \frac{1}{\sigma T^4} \frac{2\pi k_B^4 T^4}{h^3 c_o^2} \int_{c_2/\lambda T}^{\infty} \frac{t^3}{e^t - 1} \, dt$$

When $\lambda T \to \infty$, $f = 1$ and so

$$\sigma T^4 = \frac{2\pi k_B^4 T^4}{h^3 c_o^2} \underbrace{\int_0^{\infty} \frac{t^3}{e^t - 1} \, dt}_{\equiv \zeta(4)\Gamma(4)}$$

where $\Gamma(4) = 3!$ and $\zeta(4)$ is the Riemann zeta function (Euler: $\zeta(4) = \pi^4/90$).

$$\begin{aligned} f(\lambda T) &= \frac{15}{\pi^4} \int_0^{\infty} \frac{t^3}{e^t - 1} \, dt - \frac{15}{\pi^4} \int_0^{c_2/\lambda T} \frac{t^3}{e^t - 1} \, dt \\ &= 1 - \frac{15}{\pi^4} \Gamma(4) \, \zeta(X, 4) = 1 - \frac{90}{\pi^4} \zeta(X, 4) \end{aligned}$$

where $X = c_2/\lambda T$, and $\zeta(X, s)$ is the incomplete zeta function.

Integration of directional emissivity for alumina

$$\varepsilon(\lambda, T) = \int_0^{\pi/2} \varepsilon'(\theta, \lambda, T) \sin(2\theta)\, d\theta$$

Data in 12° increments over $0° \leqslant \theta \leqslant 72°$. Essentially constant from 0 to 36°; this range was integrated analytically. From 36° to 84° a five-point trapezoidal rule was used, and the integral from 84° to 90° was approximated as a trapezoid. The value at 90° was set to zero, in line with theory. Numerical truncation error is 1.0% for a gray surface.

Integration of directional emissivity for alumina

$$\varepsilon(\lambda, T) = \int_0^{\pi/2} \varepsilon'(\theta, \lambda, T) \sin(2\theta)\, d\theta$$

Data in 12° increments over $0° \leqslant \theta \leqslant 72°$. Essentially constant from 0 to 36°; this range was integrated analytically. From 36° to 84° a five-point trapezoidal rule was used, and the integral from 84° to 90° was approximated as a trapezoid. The value at 90° was set to zero, in line with theory. Numerical truncation error is 1.0% for a gray surface. The data showed angular behavior consistent with a dielectric. On this basis, interpolated using a value representative of large angle for a dielectric: $\varepsilon(84°, \lambda) \approx 0.75\, \varepsilon(72°, \lambda)$.

Integration of directional emissivity for alumina

$$\varepsilon(\lambda, T) = \int_0^{\pi/2} \varepsilon'(\theta, \lambda, T) \sin(2\theta) \, d\theta$$

Data in 12° increments over $0° \leqslant \theta \leqslant 72°$. Essentially constant from 0 to 36°; this range was integrated analytically. From 36° to 84° a five-point trapezoidal rule was used, and the integral from 84° to 90° was approximated as a trapezoid. The value at 90° was set to zero, in line with theory. Numerical truncation error is 1.0% for a gray surface. The data showed angular behavior consistent with a dielectric. On this basis, interpolated using a value representative of large angle for a dielectric: $\varepsilon(84°, \lambda) \approx 0.75\, \varepsilon(72°, \lambda)$. Without more data, cannot exclude peak emissivity above 80° predicted by Drude's model for metals; but sensitivity analysis letting $\varepsilon(84°, \lambda) \approx 2.5\, \varepsilon(72°, \lambda)$ increases the hemispherical emissivity by only about 5% of the previous estimate.

Nondimensional results for model surfaces

$\varepsilon^i(T_m)$ excellent for $T_2/T_1 = 1 \pm 30\%$ or more

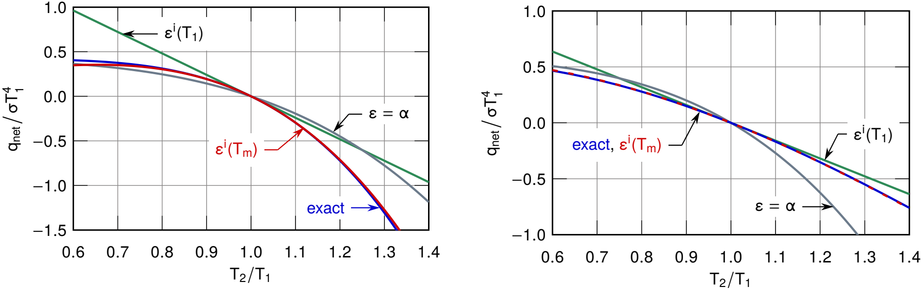

Model surfaces: $\alpha(T_1, T_2)$ has strong dependence on T_2

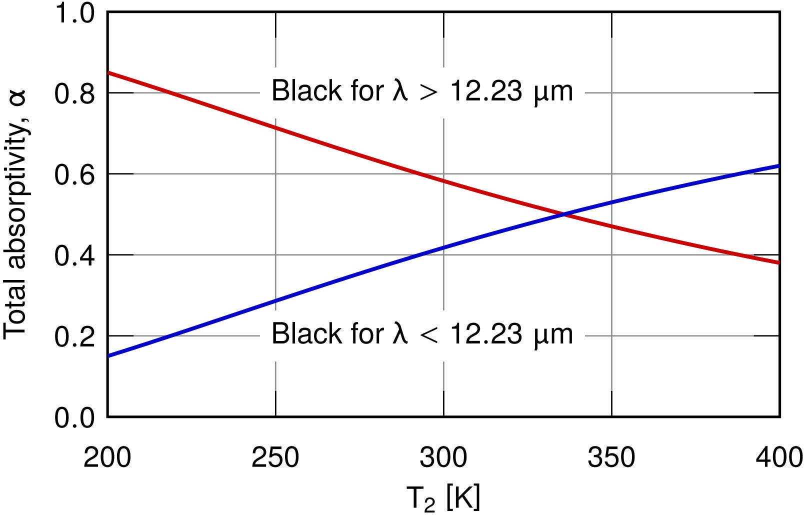

The constant X_z, the finite solution of $dF/dX = 0$

$$4\left(1 - e^{-X_z}\right) = X_z$$

In terms of the Lambert *W* function

$$X_z = 4 - W\left(4e^{-4}\right) = 3.92069\cdots$$

X_z is irrational. Diophantine approximation by continued fractions:

$$X_z = 3.92069\cdots = 3 + \cfrac{1}{1 + \cfrac{1}{11 + \cfrac{1}{\ddots}}}$$

Successive convergents give rational approximations:

$$X_z \approx \left\{4, \frac{47}{12}, \ldots, \frac{149}{38}, \frac{247}{63}, \ldots, \frac{1137}{290}, \ldots\right\}$$ 2^{nd} one is within 0.1%